Journal of Sound and Vibration (1999) **228**(1), 199–210
Article No. jsvi.1999.2420, available online at http://www.idealibrary.com on IDEAL®

LETTERS TO THE EDITOR

ON THE CROSS WAVELET ANALYSIS OF DUFFING OSCILLATOR

A. KYPRIANOU AND W. J. STASZEWSKI

Dynamics Research Group, Department of Mechanical Engineering, University of Sheffield, Mappin Street, Sheffield S1 3JD, England

(*Received* 22 *March* 1999, *and in final form* 16 *June* 1999)

1. INTRODUCTION

There are many types of non-linearities which display a wide-varying nature of restoring forces and natural frequencies of a system. The varying nature of the vibration can be analyzed using different time–frequency and time–scale approaches. This includes the application of the Hilbert transform [1, 2], Wigner–Ville distribution [3], Gabor transform [4] and wavelets [5–8].

Most of the work done in this area is based on an impulse excitation and therefore utilize only the system response. Although the classical input–output analysis given by the frequency response function (FRF) is well known and established for linear systems, it requires an extension for non-linear and non-stationary processes. The first few attempts include the generalized FRF based on evolutionary spectrum [9] and wavelet [10] approach.

The results given by these techniques are still limited. The object of the current paper is to show that *cross-wavelet* analysis can give new insights with respect to the input–output system identification.

2. CROSS-WAVELETS

One of the aims of this paper is to give an interpretation of the cross wavelet. The authors found that this is better achieved using the Riesz Representation theorem in Hilbert function spaces to explain wavelet analysis. Very briefly, a function space is a vector space whose member components are functions of time or of a discrete index. It is well known that the mother wavelet $\psi(t)$ generates a family of wavelets indexed by scale a and translation b as follows:

$$\psi_{a,b} = \frac{1}{\sqrt{a}}\psi\left(\frac{t-b}{a}\right). \tag{1}$$

This vector family can be used to analyze a time signal $\mathbf{X}(t)$, by taking the function–space inner product of each member $\psi_{a,b}(t)$ with $\mathbf{X}(t)$; the result of the

0022-460X/99/460199 + 12 $30.00/0

wavelet transform. The wavelet transform $W_{a,b}(\mathbf{X})$ can be defined as [11]

$$W_{a,b}(\mathbf{X}) = \int_{-\infty}^{\infty} \bar{\psi}_{a,b}(t)\mathbf{X}(t)\,\mathrm{d}t = \langle \psi_{a,b}, \mathbf{X} \rangle = \psi_{a,b}^{*}\mathbf{X}. \tag{2}$$

The importance of this equation is that it represents that inner product in Hilbert space as the operation of the adjoint wavelet $\psi_{a,b}^{*}$ on the analyzed vector $\mathbf{X}$. This emphasizes that the inner product (2) is an operator which transforms $\mathbf{X}$ into a scalar. This is the component of $\mathbf{X}$ appeared in the synthesized (reconstruction) formula with the dual wavelet $\psi^{\alpha,b}$. The reconstruction formula has a meaning only when the wavelet function $\psi_{\alpha,b}(t)$ satisfies appropriate admissibility conditions [12].

For any two time signals, the input $\mathbf{X}$ and the output $\mathbf{Y}$ of a system, the cross wavelet transform is the inner product of the output $\mathbf{Y}$ with a transformed version of the input $\mathbf{X}$:

$$\bar{W}_{a,b}(\mathbf{Y})W_{a,b}(\mathbf{X}) = \langle \overline{\psi_{a,b}\mathbf{Y}} \rangle \langle \psi_{a,b}\mathbf{X} \rangle = \mathbf{Y}^{*}\psi_{a,b}\psi_{a,b}^{*}\mathbf{X} = \langle \mathbf{Y}, \psi_{a,b}\psi_{a,b}^{*}\mathbf{X} \rangle. \tag{3}$$

Here $\psi_{a,b}\psi_{a,b}^{*}$ is the transformation operator. Therefore, the cross analysis can be interpreted as taking the inner product of the output $\mathbf{Y}$ with a transformed version of the input $\mathbf{X}$. The effect of this transformation on $\mathbf{X}$ can be studied following the space projection:

$$C^{R} \xrightarrow{\psi_{a,b}^{*}} C \xrightarrow{\psi_{a,b}} C^{R}, \tag{4}$$

where C^{R} denotes the space of all time signals able to undergo wavelet transformation and C is the field of scalar complex numbers.

This projection shows that $\psi_{a,b}^{*}$ firstly calculates the components $W_{a,b}$ of the signal $\mathbf{X}$ with respect to the dual wavelet $\psi^{a,b}$ and then multiplies it with $\psi_{a,b}$. The entire operation yields a new vector in C^{R} which, is considered to be the projection of $\mathbf{X}$ parallel to the wavelet $\psi_{a,b}$. The value of $W_{a,b}$ indicates the shrinkage or enlargement of $\psi_{a,b}$. Therefore, the projection given by equation (4) identifies the amount of $\psi_{a,b}$ in $\mathbf{X}$, or the amount of $\mathbf{X}$ at scale a and translation b. The inner product of this vector with $\mathbf{Y}$ gives the similarity of $\mathbf{Y}$ with the projected component of $\mathbf{X}$ at scale a and translation b onto the vector $\psi_{a,b}$. Equation (3) asserts that the inner product is the cross-wavelet analysis of the corresponding wavelet transforms.

A similar analysis as above, reveals the similarity between the cross-wavelet analysis and the classical FRF. The use of complex exponential functions $\mathrm{e}^{\mathrm{j}\omega t}$, instead of the wavelets $\psi_{a,b}$, in equation (2) results the Fourier transform of a signal $\mathbf{X}$:

$$\mathbf{X}(\omega) = \langle \mathbf{e}_{\omega}, \mathbf{X} \rangle = (\mathbf{e}_{\omega})^{*}\mathbf{X}, \tag{5}$$

where the complex exponentials $e^{j\omega t}$ are indexed by the angular frequency ω. The ratio of $\mathbf{Y}(\omega)$ to $\mathbf{X}(\omega)$ is the classical FRF:

$$\mathrm{FRF}(\omega) = \frac{\langle \mathbf{e}_\omega, \mathbf{Y} \rangle}{\langle \mathbf{e}_\omega, \mathbf{X} \rangle} = \frac{(\mathbf{X})^* \mathbf{e}_\omega (\mathbf{e}_\omega)^* \mathbf{Y}}{(\mathbf{X})^* \mathbf{e}_\omega (\mathbf{e}_\omega)^* \mathbf{X}}. \tag{6}$$

Using equation (3), FRF can be expressed as the cross analysis of the Fourier transforms

$$\mathrm{FRF}(\omega) = \frac{\overline{\mathbf{X}(\omega)}\mathbf{Y}(\omega)}{\mathbf{X}(\omega)^2} = \frac{\overline{\overline{\mathbf{Y}(\omega)}\mathbf{X}(\omega)}}{\mathbf{X}(\omega)^2} \tag{7}$$

This is an alternative way of representing the classical FRF. By virtue of equation (7), it can be seen that the frequency response is the normalized similarity between the input and the projection of the output parallel to the wave $\mathbf{e}_\omega$. The normalization is given by the energy of $\mathbf{X}$ at frequency ω.

The frequency response function however, gives only information in frequency domain ignoring the time at which each frequency component occurs. On this ground, a function similar to a time-varying FRF can be defined utilizing the cross wavelet analysis of equation (3). Therefore, one can define a scale, translation response function as

$$\mathrm{STRF}(\alpha, b) = \frac{\overline{W_{\alpha,b}(\mathbf{X})} W_{\alpha,b}(\mathbf{Y})}{(W_{\alpha,b}(\mathbf{X}))^2} = \frac{\overline{\overline{W_{\alpha,b}(\mathbf{X})} W_{\alpha,b}(\mathbf{Y})}}{(W_{\alpha,b}(\mathbf{X}))^2}. \tag{8}$$

Equation (8) can be interpreted as follows; firstly, it breaks the output into wavelet of scale α and translation b and enlarges or shrinks it by an amount that it would have been used by reconstruction formula [12]. This wavelet is further used to identify its similarity with the input at same scale and translation. Inducing from the classical FRF, the maxima of this similarity should coincide with resonances in the system. Any spread around them over the translation and scale plane should give an indication of the time-varying damping of the system.

3. RESULTS

The Duffing oscillator is one of the bench marks for non-linear analysis. It is also used here for a comparative cross-wavelet study with a linear single-degree-of-freedom system using the cross-wavelet analysis. The equation of motion of Duffing oscillator used is given by

$$\ddot{y} + 10\dot{y} + 10^4 y + 10^6 y^3 = x, \tag{9}$$

whereas that of the linear system by

$$\ddot{y} + 10\dot{y} + 10^4 y = x. \tag{10}$$

Both of the oscillators are considered to consist of 1 kg mass, 10 Ns/m damping and 10^4 N/m of linear stiffness. The Duffing oscillator in addition includes a 10^6 N/m^3 cubic stiffness.

The FRFs of the Duffing and linear oscillator are shown in Figures 1 and 2 respectively. The input used in the analysis is a chirp signal shown in Figure 3(a). Because of its frequency sweeping nature it is widely used for vibration testing. A controlled frequency band of chirps allows for the response time history able to show the structural resonances. Their mathematical wavelet analysis is given in reference [13]. The chirp signal shown at Figure 3(a) starts at frequency of 5 Hz and crosses 80 Hz in 2 s.

The mother wavelet used for this study is the Morlet wavelet defined by the following function:

$$\psi(t) = e^{j\omega_0 t} e^{-t^2/2}. \tag{11}$$

The wavelet transform is not related explicitly with any of the conventional time–frequency signal decomposition methods. Nevertheless, a relationship

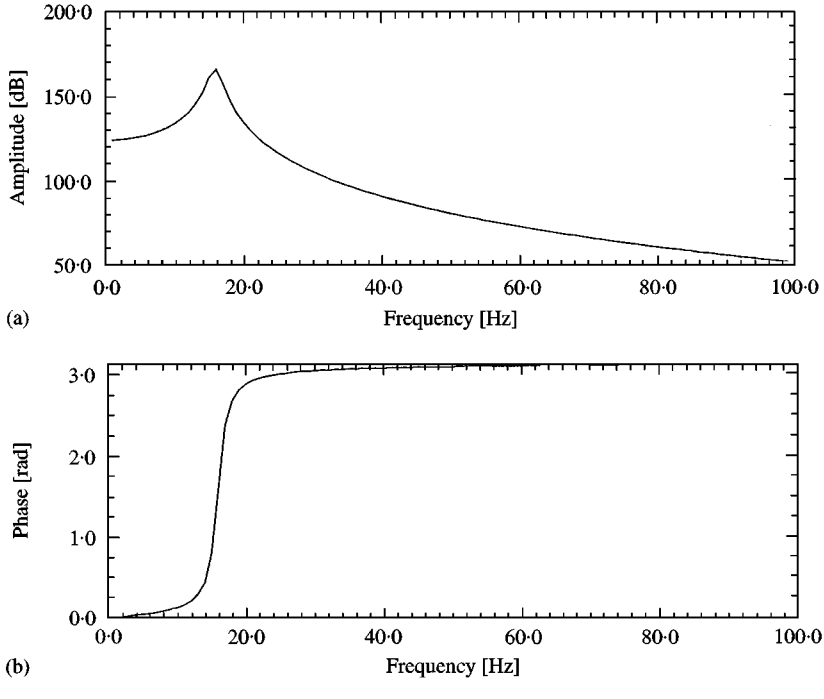

Figure 1. Frequency response function of the linear oscillator: (a) Amplitude, (b) phase.

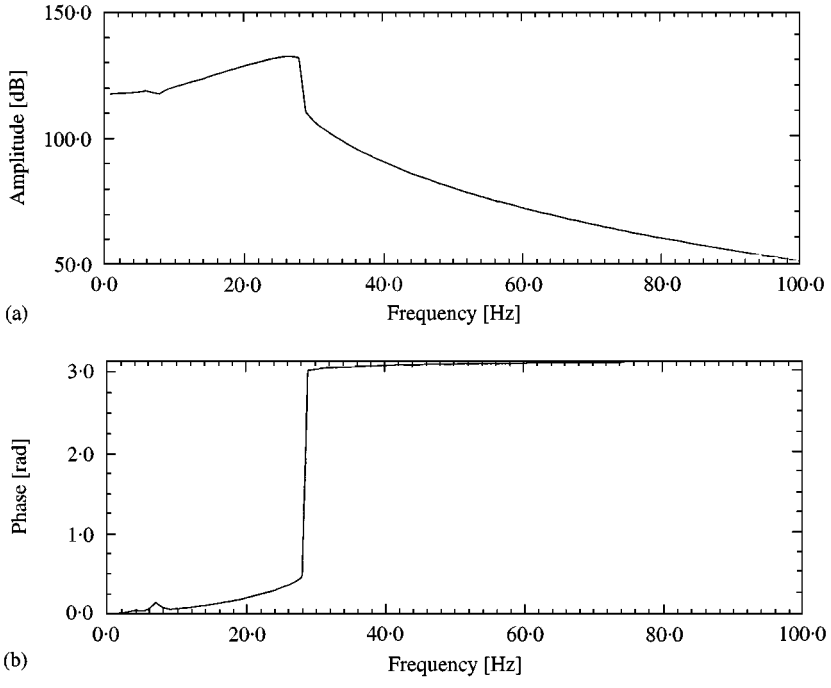

Figure 2. Frequency response function of the Duffing oscillator: (a) Amplitude, (b) phase.

between the scale and frequency can be given by [14]

$$a_f = \frac{\omega_0 f_s}{2\pi f_w} \frac{1}{f_x}, \tag{12}$$

where a_f is the scale value at which, the wavelet filter centres when analyzing the signal frequency f_x, f_s denotes the sampling frequency of the analyzing signals whereas f_w is the sampling frequency of the wavelet. Both sampling frequencies for this study were taken to be 500 Hz each. The base angular frequency ω_0 of the Morlet wavelet was chosen to be $1{\cdot}75\pi$ rad/s, so this value satisfies the wavelet admissibility condition. The wavelet transform has been calculated over 200 scales starting from a minimum scale value of 0·0035.

The time history of the response of the linear and non-linear system is shown in Figures 3(a) and 3(b) respectively. Figure 4 shows the wavelet transform of the input chirp signal. Here, the continuous frequency ranges 5–80 Hz can be observed. The wavelet transform of the linear system in Figure 5 shows that the response is mainly around the logarithmic scale of 1·2 (13·86 Hz)–1·3 (17·46 Hz). These frequencies correspond to the working bandwidth of the system around the resonance of 15·55 Hz.

Figure 6 shows the wavelet transform of the Duffing oscillator response. In Figure 3(c) the sudden increase in dilation at 0·9 s of the Duffing oscillator time

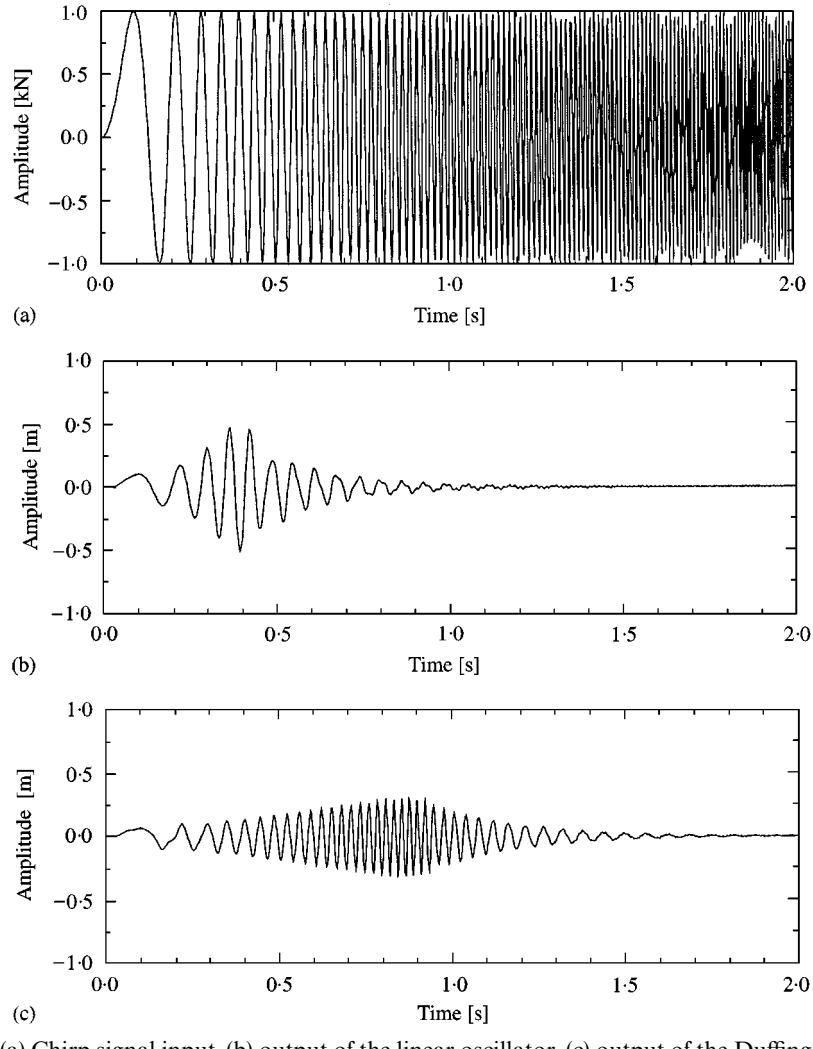

Figure 3. (a) Chirp signal input, (b) output of the linear oscillator, (c) output of the Duffing oscillator.

response indicates that the output frequency does not follow the input frequency. In the wavelet transform domain of Figure 6 this shows up as a sudden decrease of the scale.

The cross-wavelet analysis between the output **Y** of the system and the input **X** is shown in Figure 7 for the linear and in Figure 8 for the non-linear system. In Figures 7(a) and 8(a) the 3-D plots of the magnitude of the cross-wavelet transform is shown. It is clear that this gives the overall information about the system in both time and frequency domain. If one takes cross-sections across the translation axis it will reveal the scale (frequency) response function at that time. Therefore, information about the frequency characteristics at that time will be evident. Any high values mean that the system at that time instant is responding vividly to an input with the corresponding scales. Next taking cross-sections across the scale

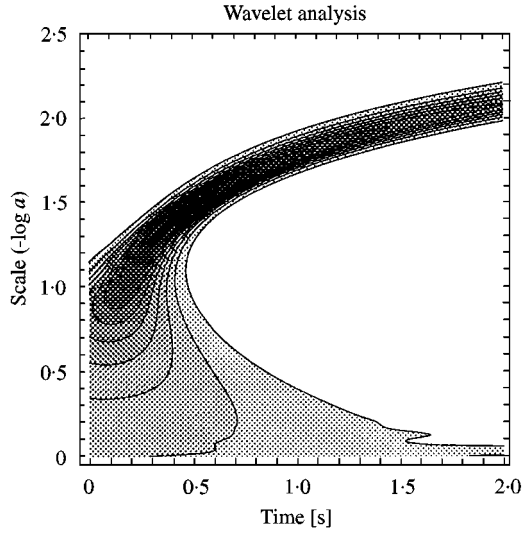

Figure 4. Wavelet transform of the chirp input.

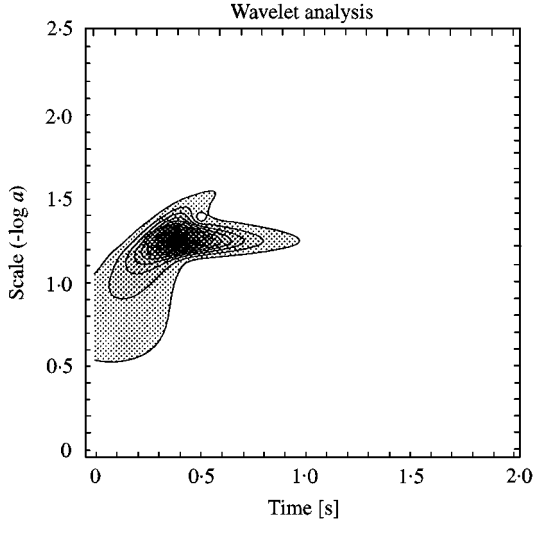

Figure 5. Wavelet transform of the linear oscillator output.

axis, information is available about the evolutionary response of the system to the input at that scale. The cross-wavelet contour plots are shown in Figures 7(b) and 8(b) for the linear and Duffing oscillator respectively. They can be utilized to observe the effect of non-linearity in terms of the varying input frequency content; one can use equation (12) to obtain the corresponding frequency at the scale of the observation.

Here, the cross-wavelet transform enhances the similarities between the wavelet transforms of the input and output. The fact that the input is used is an advantage

over the continuous wavelet transform methods used in the past, where the analysis of the impulse response of the non-linear system was used [7, 15]. It is known that, because of its time localization, an impulse input does not excite the higher order frequencies of non-linear system. As a consequence a more general signal that is well spread in time and frequency can be used. In such a case, the FRF reveals information as the system was excited by a single harmonic all the time and responds with a simple harmonic all the time. This means that any existing sub-resonance frequencies or super-resonance frequencies can only be interpreted as being due to a single harmonic input of the same frequency. Cross-wavelet

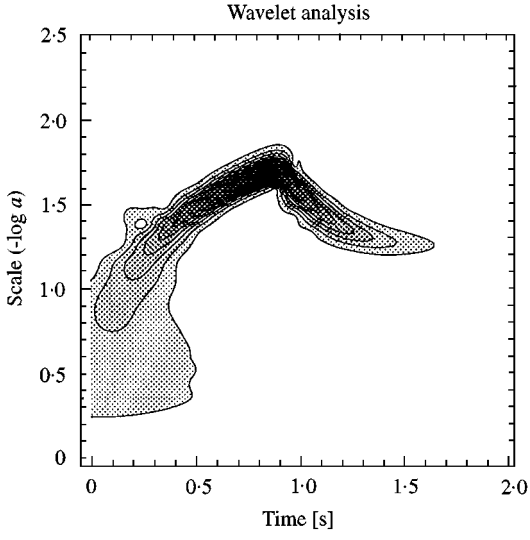

Figure 6. Wavelet transform of the Duffing oscillator output.

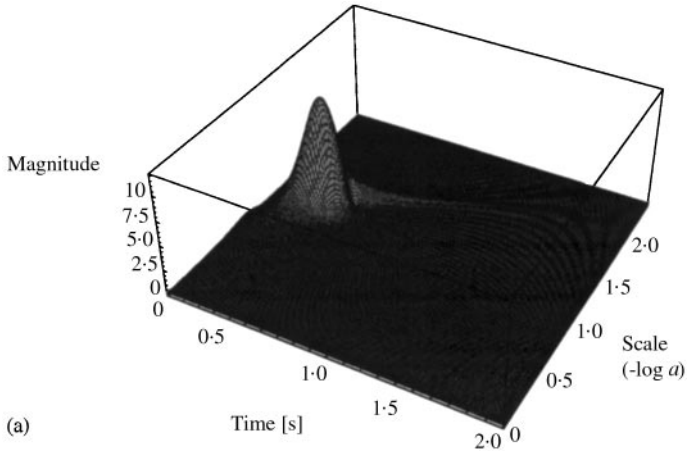

Figure 7. Cross-wavelet analysis of linear oscillator: (a) Amplitude, (b) amplitude contour plot and (c) phase.

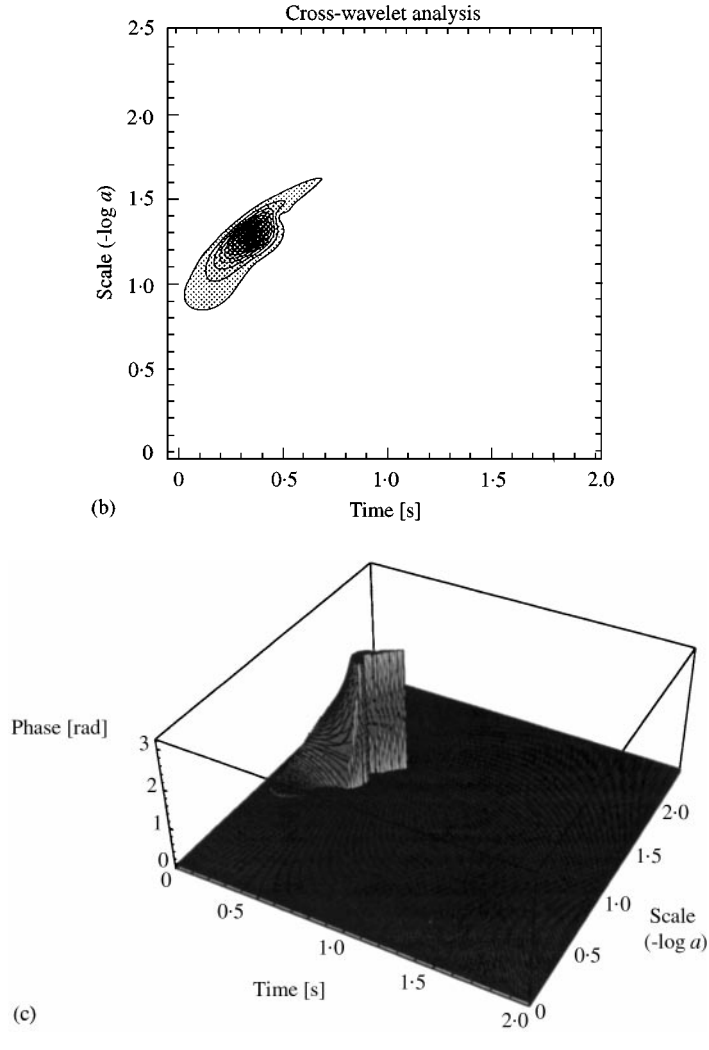

Figure 7. Continued.

circumvents this problem by localizing the similarities of the input and the output at different scales (frequencies). This indicates whether the response is the outcome: (a) of an input with the same spectral characteristics (case of high values of cross-wavelet) or (b) due to the non-linear structure responding on a previous input with different spectral characteristics. On these grounds when the wavelet transform of the output of the Duffing oscillator for Figure 6 is compared with cross-wavelet amplitude of Figure 8(b) it can be deduced that the response after the first second is because of the non-linearity. It is portrayed by the zero magnitude of the cross-wavelet plot after the first second as it does not register any similarity with the input.

Figures 7(c) and 8(c) show the phase difference of the cross-wavelet analysis over the translation scale plane. This gives time-localized information about the lag of

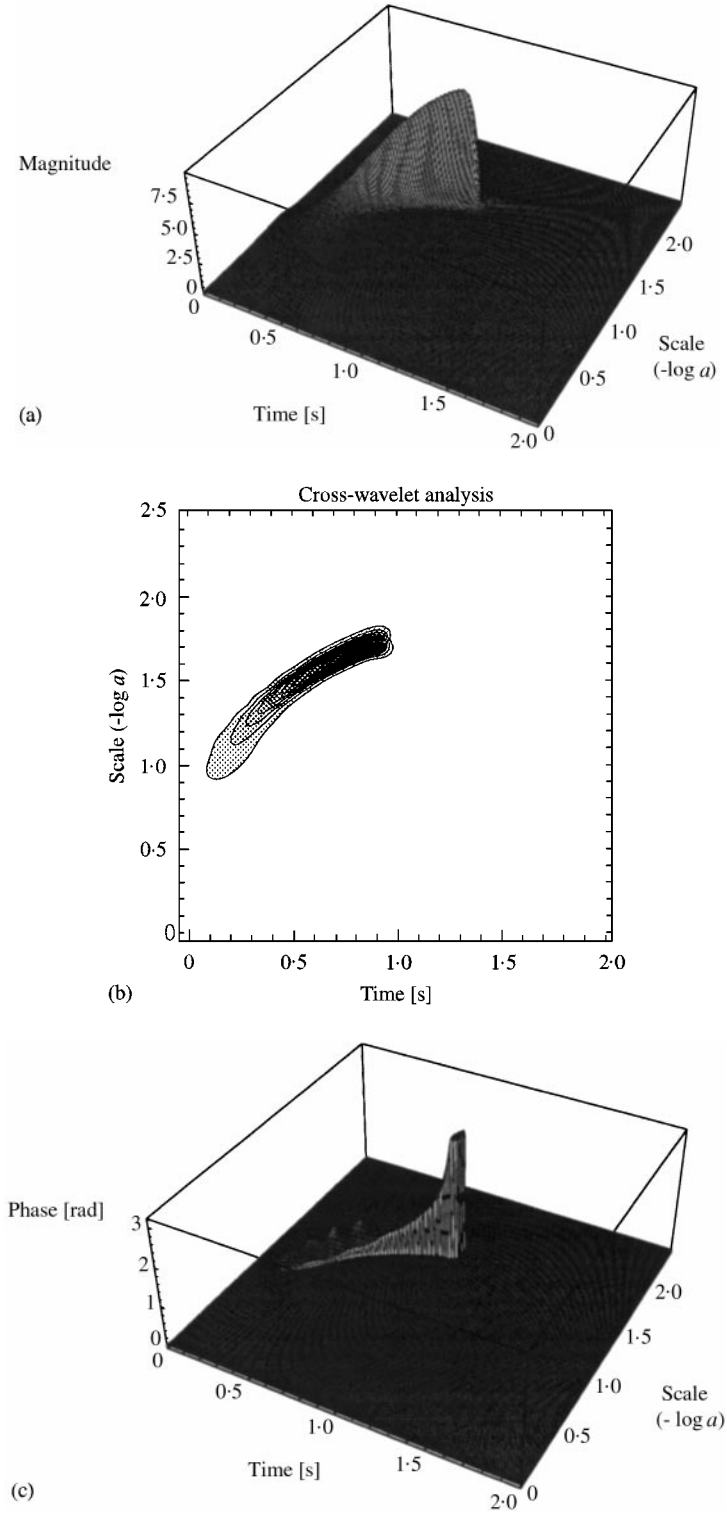

Figure 8. Cross-wavelet analysis of Duffing oscillator: (a) Amplitude, (b) amplitude contour plot and (c) phase.

output to the input at a specified scale. A proper utilization of this information can identify modal characteristics of the system. Any resonances can be identified by 180° phase difference and damping can be identified by the rate of change of the phase across the scales.

4. CONCLUSION

The cross-wavelet analysis has been used as an alternative approach to classical input–output analysis based on the FRF. This study shows the similarities and differences between these two approaches. A simple Duffing oscillator example shows that the cross-wavelet analysis is able to characterize a system in both time and scale domains and therefore reveal its varying time–frequency nature. More work is required to fully utilize the potential of the cross-wavelet analysis to the study of non-linear systems.

ACKNOWLEDGMENT

The authors would like to express their gratitude to Dr Keith Worden for valuable comments and discussion.

REFERENCES

1. M. Feldman 1994 *Mechanical Systems and Signal Processing* **8**, 119–127. Non-linear system vibration analysis using Hilbert transform—I free vibration analysis method 'Freevib'.
2. M. Feldman 1994 *Mechanical Systems and Signal Processing* **8**, 309–318. Non-linear system vibration analysis using Hilbert transform—II forced vibration analysis method 'Forcevib'.
3. F. Brancaleoni, D. Spina and C. Valente 1993 *Safety Evaluation Based on Identification Approaches*. (H. G. Natke, G. R. Tolmison, J. T. P. Yao, editors), 276–291. Braunschweig/Wiesbaden, Germany. Vieweg International Scientific Book Series. Damage assessment from the dynamic response of deteriorating structures.
4. D. Spina, C. Valente and G. R. Tomlinson 1996 *Nonlinear Dynamics* **11**, 235–254. A new procedure for detecting nonlinearity from transient data using the Gabor transform.
5. D. Permann and I. Hamilton 1992 *Physical Review Letters* **69**, 2607–2610. Wavelet analysis of time series for the duffing oscillator. the detection of order within chaos.
6. W. J. Staszewski 1997 *Journal of Sound and Vibration* **203**, 283–305. Identification of damping in MDOF systems using time-scale decomposition.
7. W. J. Staszewski 1998 *Journal of Sound and Vibration* **214**, 639–658. Identification of non-linear systems using multi-scale ridges and skeletons on the wavelet transform.
8. W. J. Staszewski 1998 *The Shock and Vibration Digest* **30**, 457–472. Structural and mechanical detection using wavelets.
9. M. B. Priestley 1998 *Non-Linear and Non-Stationary Time Series Analysis*. London: Academic Press.
10. W. J. Staszewski and J. Giacomin 1997 *Proceedings of the 15th International Modal Analysis Conference—IMAC*, *Orlando*, *Florida*, Vol **1**(4), 425–431. Application of the wavelet based FRFs to the analysis of nonstationary vehicle data.
11. G. Kaiser 1994 *A Friendly Guide to Wavelets*. Boston: Birkhäuser.

12. I. Daubechies 1992 *Ten Lectures on Wavelets*. Philadelphia: SIAM.
13. Y. Meyer and H. Xu 1997 *Applied and Computational Harmonic Analysis*, **4**, 366–379. Wavelet analysis and chirps.
14. W. J. Staszewski 1998 *Mechanical Systems and Signal Processing* **8**, 289–307. Application of the wavelet transform to fault detection in a spur gear.
15. W. J. Staszewski and G. R. Tomlinson 1994 *The 19th International Conference in Structural Dynamics and Modal Analysis*, 371–377. Fault detection procedures employing the wavelet transform.